INDIAN STREAMS RESEARCH JOURNAL

ISSN: 2230-7850
IMPACT FACTOR : 5.1651 (UIF)
VOLUME - 7 | ISSUE - 2 | MARCH - 2017

MULTI-AGENT COLLABORATIVE PATH PLANNING ALGORITHM WITH MULTIPLE MEETING POINTS

Dr Rekha
Assistant professor in Electronics Government College (Autonomous)
Kalaburagi

Abstract: Due to the single-agent-single-task arrangement, traditional multi-agent path planning methods frequently result in path overlap and excessive energy usage while handling cooperative tasks. The "many-to-one" cooperative planning approach has been suggested as a result, and while it has improved, it still has issues with the large search space for meeting places and irrational job transfer locations. In order to accomplish multi-agent path planning with task handovers at multiple or single meeting points, this work introduces the Cooperative Dynamic Priority Safe Interval Path Planning with a multi-meeting-point and single-meeting-point solving mode switching (Co-DPSIPPms) algorithm. Firstly, the positional relationships among agents in the cooperative group are used to define the initial priority. Multiple meeting places are swiftly located using the improved Fermat point method. Secondly, taking into account that

Keywords: multi-agent; task handover; multiple meeting points; safe intervals; many-to-one collaboration; segmented path planning.

1. Introduction

The multi-agent path planning problem, commonly referred to as multi-agent path finding (MAPF), has drawn a lot of attention as a primary area of robotics research. Several academics have put out various multi-agent path planning algorithms [2-4]. Numerous domains, including intelligent transportation [5-7], warehouse logistics [8–10], emergency response [11], express sorting, and numerous others [12,13], have seen the successful use of these algorithms.

Priority-based and non-priority-based multi-agent path planning algorithms can be generally classified according to whether or not agents need to be arranged in a predetermined planning sequence. Priority-based path planning algorithms include Hierarchical Cooperative A* (HCA*) algorithms [15] and those that use Safe Interval Path Planning (SIPP) as the fundamental search mechanism for multi-agent path planning [14]. Conversely,

both of which leverage the SIPP as the foundation for single-agent planning, ensuring a rapid solution speed while providing high-quality, collision-free path plans. In the realm of non-priority-based algorithms, CBS particularly stands out. It discovers collision-free paths for multiple agents through conflict search and resolution, with the capability to find optimal and complete solutions. However, the solution efficiency of CBS is closely tied to the desired solution quality, with higher quality demands often accompanied by more constraints and slower solution speeds. In response, Barer et al. successively proposed Enhanced CBS (ECBS) [21] and Improved CBS (ICBS) [22], further enhancing the algorithms' solution efficiency.

As task complexity continues to increase, multi-agent collaboration has emerged as a pivotal approach for efficiently accomplishing tasks. Consequently, a deeper exploration of multi-agent cooperative path planning techniques for multiple cooperative agent groups is paramount, particularly focusing on the critical aspect of task handovers. Given that single- meeting-point task handover strategies tend to lead to path redundancy and inefficiency, this paper innovatively proposes the Cooperative Dynamic Priority Safe Interval Path Planning with a multi-meeting-point and single-meeting-point solving mode switching (Co-DPSIPP$_{ms}$) algorithm. This algorithm aims to optimize path planning and enhance task execution efficiency. Compared with the solving efficient (Explicit estimation CBS, EECBS) algorithm [23] in MAPF, the Co-DPSIPP$_{ms}$ algorithm incorporates the idea and method of multi-agent collaboration in accomplishing multiple tasks, which avoids a large number of agents to move long distances in the map area. It significantly reduces the energy expenditure of multi-agent systems. Compared with the Token Passing with the Task Swaps (TPTS) algorithm [24], which includes both pickup and delivery processes, the Co-DPSIPP$_{ms}$ algorithm, in which different types of agents work together collaboratively, not only enables multiple agents to collaborate on more complex tasks but also helps to improve the overall efficiency of the system in performing tasks. Compared with the same type of Cooperative CBS (Co-CBS) algorithm [25], the Co-DPSIPP$_{ms}$ algorithm extends the number of collaborative agents in a single group from the original 2 to more than 10, and the efficiency of the task execution can be further improved. In addition, it provides a more efficient computational method for obtaining the convergence position of the collaborative agents, which effectively shortens the running time of the algorithm. The core contributions of this paper are summarized as follows:

First, to address the task handover issue in multi-agent collaboration, a multi-meeting- point collaboration form is proposed, which comprehensively considers agent positions, task layouts, and priorities to optimize the selection of meeting points, thereby reducing energy consumption and unnecessary movements.

Second, a multi-agent segmented path planning strategy is designed, optimizing paths based on the starting points of sub-tasks and meeting points to ensure rapid task acquisition and handover. Meanwhile, a flexible solving mode switching mechanism is introduced to overcome the limitations of a single mode, enhancing the algorithm's adaptability and success rate.

Finally, through simulation experiments on benchmark maps combined with testing of real-world agent path plans, the effectiveness of the proposed algorithm is comprehensively validated, highlighting its significant advantages in improving path planning efficiency and reducing energy consumption.

Article Structure: Section 2 presents the fundamentals of the SIPP, CBS algorithms, and related research for the collaborative task path planning problem. Section 3 defines the MAPF and Co-MAPF problems. Section 4 details the specific implementation of the proposed method, including the pseudocode and flowchart of the entire algorithm. Section 5 describes the experimental parameter settings, results, and analysis. Section 6 validates the feasibility of the algorithm solution through real-world experiments. Section 7 summarizes the work and presents future outlooks.

2. Related Work

Basic Principles of the SIPP and CBS Algorithms

As depicted in Figure 1, the SIPP algorithm assigns a safety interval list to each map grid, which records the agent's occupancy information. When an agent expands into these grids, it directly consults the safety interval list to determine whether the grid can be occupied and the earliest possible time for occupation. The introduction of safe intervals significantly enhances the algorithm's search efficiency.

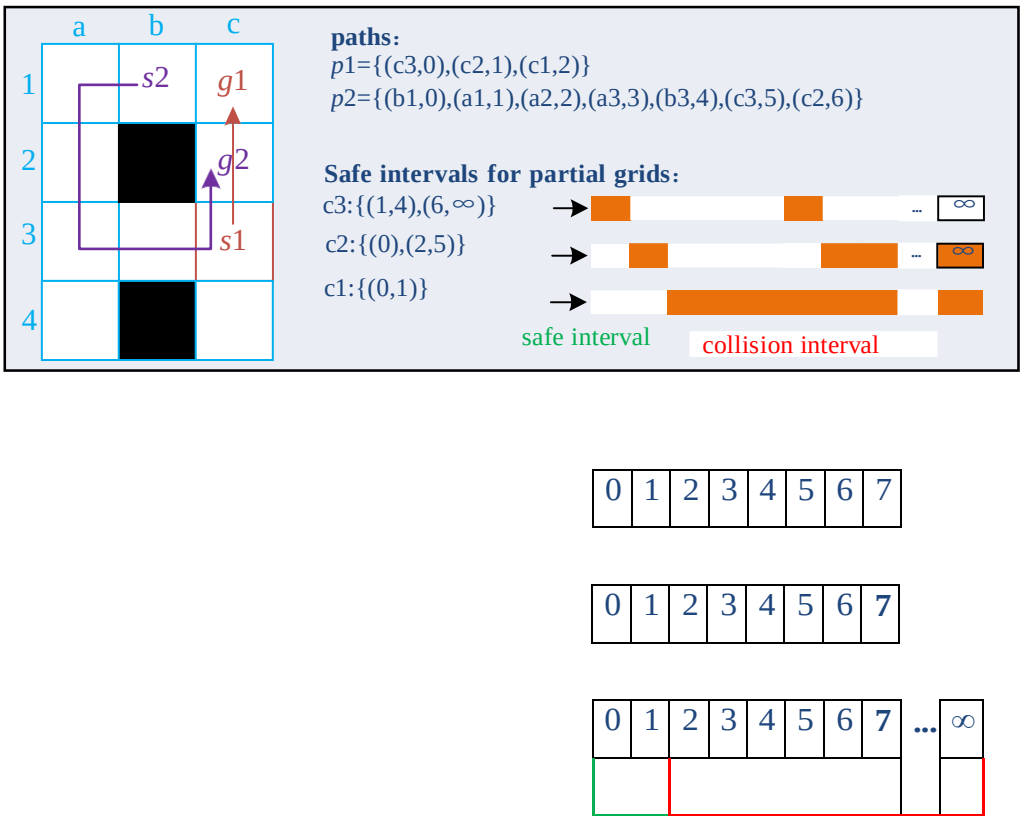

Figure 1. Principle of the SIPP algorithm.

As shown in Figure 2, the CBS plans collision-free paths through a conflict-based search tree. Conflict detection is performed between every pair of agents. When a conflict is detected, the search tree splits at the conflicting location, adds constraints to the nodes, and replans the path for one of the agents. This process is repeated until collision-free paths are obtained for all the agents.

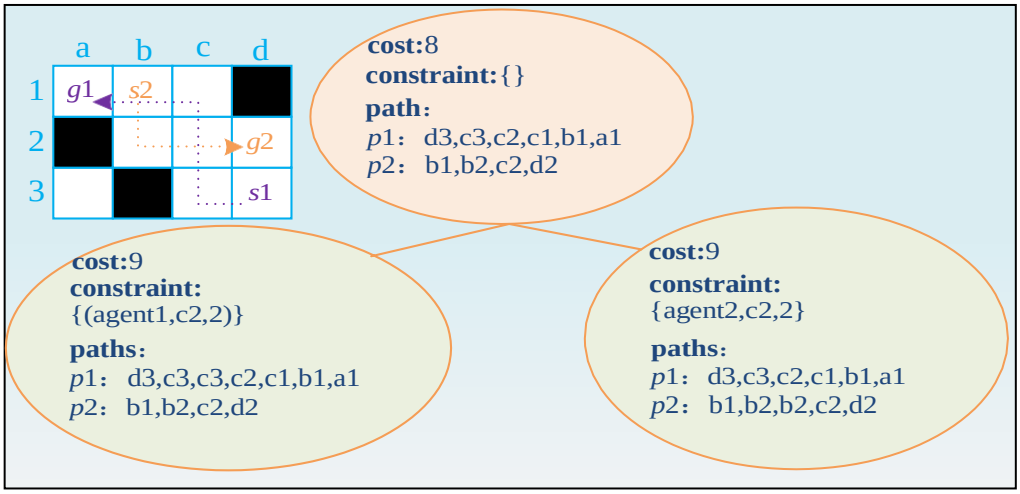

Figure 2. Principle of the CBS algorithm.

Research Progress on Multi-Agent Collaboration

In today's society, efficient task execution increasingly relies on sophisticated planning and collaboration within multi-agent systems [26,27]. Wang's team [28] addressed the chal- lenge of cooperative operation planning in unmanned farms [29] by integrating priority queues with the Dijkstra algorithm [30], achieving efficient path planning. Chen et al. [31] optimized paths for swarm unmanned aerial vehicle (UAV) reconnaissance tasks using a fast evolutionary programming genetic algorithm. Li's team [32] proposed the adaptive multi-population particle swarm optimization (AMP-PSO) algorithm to shorten paths for multi-AUV (Autonomous Underwater Vehicle) cooperative missions on the seabed. In complex environments, Zhang et al. [33] introduced the multi-objective particle swarm optimization algorithm with multi-mode collaboration based on reinforcement learning (MCMOPSO-RL), which optimizes multi-UAV collaborative paths and effectively handles.

Atia et al. [34] designed the Obstacle Guided Path Refinement (ORPG) algo- rithm to enable air–ground cooperation between UAVs and ground agents. However, these studies primarily focused on small-scale agents and tended to plan independently.

When tackling complex path planning tasks for large-scale agent systems, Grenouil- leau et al. [35] built upon the multi-agent pickup and delivery (MAPD) problem [24] by proposing the multi-label A* (MLA*) algorithm, where an agent sequentially visits multiple goal locations, significantly enhancing solution efficiency. However, this study did not involve multi-agent collaboration. Atzmon et al. [36] addressed the multi-agent rendezvous problem with the Meet in the Middle (MM*) algorithm by finding optimal meeting points for multiple agents. Motes et al. [37] combined task decomposition with task planning,

introducing the Task and Motion Planning Conflict-Based Search (TMP-CBS) algorithm to handle more complex path-planning problems. Li Jiaoyang et al. [38] proposed the Rolling-Horizon Collision Resolution (RHCR) algorithm for continuous tasks, providing an effective solution for lifelong multi-agent path-finding problems.

Other scholars are actively exploring planning methods for multi-agents collaborating on a single complex task [39–41]. However, their research often focuses on path planning within a single cooperative group, neglecting collaboration among multiple cooperative agent groups. Collaborative path planning for multiple agent groups encompasses the fol- lowing scenarios: (1) Multiple mobile charging agents replenish energy-depleted working agents, reducing travel time and energy consumption to fixed charging areas. (2) In MAPF scenarios, agent paths are optimized through deep collaboration to address path overlaps, minimize travel ranges, and reduce conflicts. (3) In warehouses, multiple sub-task agents collaborate at different workstations to deliver goods to transport agents jointly. To address the complex challenges of collaborative path planning for multiple agent groups, Greshler innovatively introduced the Co-CBS algorithm and systematically established the problem framework of Cooperative Multi-Agent Path Finding (Co-MAPF) for the first time [25]. However, given that research in the Co-MAPF field is still in its infancy, current Co-CBS algorithms mostly focus on simple collaboration scenarios involving two agents, struggling with scenarios involving multiple agents cooperating on complex tasks. The sharp contrast between the aforementioned diverse application requirements and the limitations of current research underscores the necessity and urgency of deepening the research on path planning for multi-group cooperative agents.

Problem Description

MAPF Definition

MAPF Problem Definition: In a given undirected graph $G = (V, E)$, we have a collection of agents $A = \{a_i \mid 0 < i \leq N_{robot}\}$, where each agent a_i is required to plan a collision-free path p_i from a particular starting point s_i to a goal point g_i. Figure 3 shows a schematic representation of a MAPF problem. The starting and goal points are unique for each agent, and the path p_i is represented as a series of grid node and time combinations, i.e., $p_i=\{(v_I, t_I) \mid I = 0,1, 2..., cost_i)\}$, where $cost_i$ represents the time cost required for the agent a_i to move from the starting point to the goal point.

When planning these paths, we must ensure that each agent's chosen path satisfies Equations (1)–(3) to avoid agents entering obstacle regions or having point conflicts or edge conflicts with other agents. Equation (1) indicates that at any time point t_I, no two agents can occupy the same node (point conflict). Equation (2) indicates that at any time point t_I, no two agents can traverse the same edge at the same time (edge conflict). Equation (3) requires that each node v_I in the path does not belong to the obstacle region to avoid collision. By satisfying these conditions, we can ensure that all agents can move safely and efficiently from their respective starting points to the goal point while avoiding any collision.

$$\text{s.t. } p_i \cap p_j = \varnothing \; i, j \in [1, N_{\text{robot}} \tag{1}$$

$$\{v_I = v_{J-1}\} \cap \; v_J = v_{I-1}\} = \varnothing, \; v_I \in p_i, \; v_J \in \; p_j \, I \in [0, cost_i \,], \; J \in \; 0, \; cost_j \tag{2}$$

$$v_I \notin obstacles \; v_I \in \; p_i, \; I \in [0, cost_i \,] \tag{3}$$

The optimization objective of the MAPF problem, as shown in Equation (4), is to minimize the total cost (*f lowtime*), which is the sum of the time steps required for each agent to complete its respective task. When agents require little or no waiting, the flowtime value can effectively reflect the quality of the solution.

$$f lowtime = min_{oup} \left\{ \sum_{j=1}^{k \cdot Ngr} cost_j + \sum_{i=1}^{Ngr} cost_i \right\} \tag{4}$$

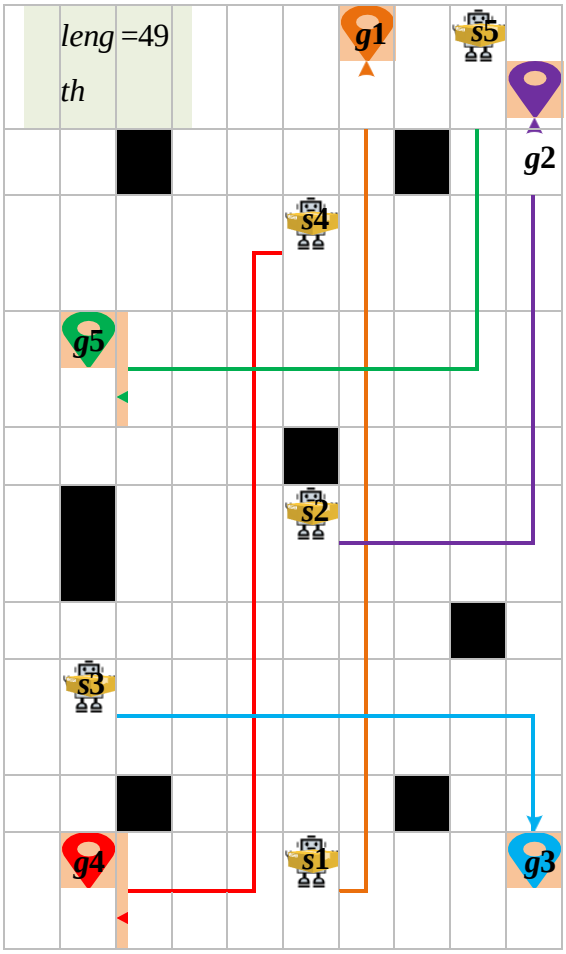

Figure 3. Schematic diagram of the MAPF problem.

2.1. Co-MAPF Description

2.1.1. Co-MAPF Definition

Co-MAPF Problem Definition: In the context of MAPF, the agents in the agent set $C = \{C_i | 0 < i \leq N_{group}\}$ work together to accomplish the tasks $tasks_i$ within their respective collaborative groups through a k-to-1 collaboration model. Each collaborative group C_i consists of k sub-tasking agents and 1 task-executing agent, i.e., $C_i = \{((a_{j1}, a_{j2}..., a_{jk}), b_j)\}$, where $(a_{j1}, a_{j2}..., a_{jk})$ represents the k sub-task agents and b_j represents the task execution agent. The collaborative task $task_i = \{(\tau_1, \tau_2..., \tau k), g\}$, where $(\tau_1, \tau_2..., \tau k)$ is the starting point of each sub-task agent and g is the common task goal point.

Taking collaborative distribution as an example, the sub-task agents start from the initial position s_i, arrive at the corresponding sub-task position τ_i to obtain the goods and then arrive at the meeting point m_i to carry out the handover of the goods with the task execution agents. After all the sub-task agents complete the handover of the goods, the task execution agent delivers these goods to the final goal point g.

For the Co-MAPF problem, the core of the solution lies in planning collision-free paths for sub-task and task-executing agents under the constraints of the MAPF. Considering the difference between the Co-

MAPF problem and the general MAPF problem regarding agent behavior during task execution, the task-executing agents need to reach the task handover location and complete the task handover with the sub-task agents before moving to the goal location. Using $f\ lowtime$ as the optimization objective poses the following issues: First, all permutations and combinations of task handover locations and handover times lead to the need to consume a large amount of computational resources to obtain the least time-costly task meeting point, which makes it difficult to provide timely and effective solutions in complex scenarios. Furthermore, optimizing with $f\ lowtime$ as the objective tends to result in longer paths, higher energy consumption, and reduced task volume due to frequent charging, ultimately impacting overall efficiency. Therefore, this paper adopts the total path length (*length*) as the primary optimization objective, as shown in Equation (5) ($pathlength_i$ is the path of agent i), aiming to find a solution with a shorter total length of paths for all agents. This approach aims to reduce energy consumption during actual execution and enhance the system's overall efficiency.

$$length = min\ \{ \sum_{j=1}^{N_{group}} pathlength_{h_j} + \sum_{i=1}^{N_{group}} pathlength_i \} \quad (5)$$

2.1.2. Two Forms of Collaborative Task Handover

When addressing the Co-MAPF problem, the variability of task handover locations and the number of these locations (meeting points) significantly impact the planning outcomes. Therefore, selecting an appropriate strategy to determine the optimal number of meeting points is crucial for obtaining high-quality solutions.

As shown in Figure 4, when adopting the collaboration form with a single meeting point, each set of cooperative task agents must reach a unique meeting point for their group to perform task handovers. This handover form is simple and direct, requires few computational resources, and can be solved using the Cooperative Dynamic Priority SIPP with a single meeting point (Co-DPSIPP$_s$) algorithm.

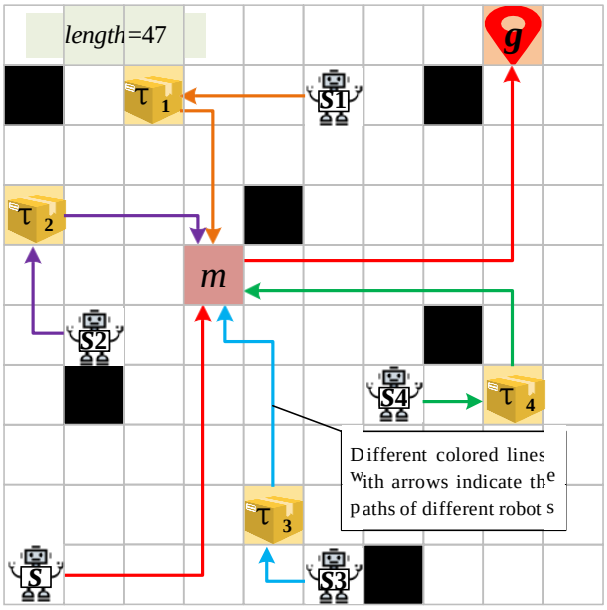

Figure 4. Collaborative form of single-meeting-point (Co-DPSIPP$_S$).

However, using a single meeting point for all task handovers can result in some sub- task agents needing to carry tasks and travel longer distances to reach point *m*, where the tasks are then transferred to the final destination point *g*, generating longer redundant paths. Therefore, a better solution can be obtained by adopting the collaboration form with multiple meeting points for task handovers, as illustrated in Figure 5. Naturally, the computational process for multiple meeting points is more complex than for a single one. This problem can be solved using the Cooperative Dynamic Priority SIPP with multiple meeting points (Co-DPSIPP$_m$) algorithm.

Considering the characteristics of single-meeting-point and multi-meeting-point solv- ing modes, this paper proposes a Cooperative Dynamic Priority SIPP with a multi-meeting- point and single-meeting-point solving mode switching (Co-DPSIPP$_{ms}$) algorithm. The algorithm combines the advantages of both multi-meeting-point and single-meeting-point solving modes, allowing the algorithm to switch to single-meeting-point solving mode.

when the multi-meeting-point solving mode is in trouble. This approach enhances the algorithm's success rate and meets the demands of complex collaborative tasks.

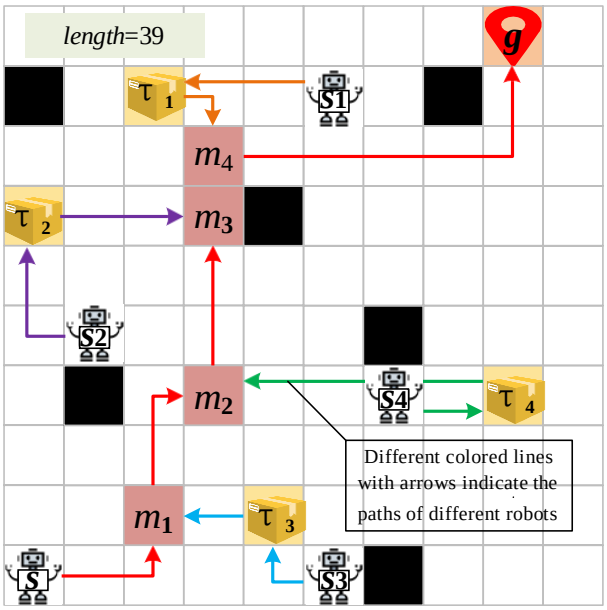

Figure 5. Collaborative form of multi-meeting-point (Co-DPSIPP$_m$).

3. Co-DPSIPP$_{ms}$ Algorithm

Given the NP-hard nature of the Co-MAPF problem [42], producing effective paths within a limited time frame is often challenging using optimal algorithms directly in complex environments. Consequently, researchers have shifted their focus to exploring suboptimal algorithms [16,19–21], aiming to obtain suboptimal solutions that meet system requirements rapidly. Building upon SIPP as the fundamental path-planning strategy, this paper innovatively proposes a suboptimal path-planning algorithm that achieves efficient collaboration at multiple or single meeting points, thereby swiftly outputting optimized path solutions.

Multiple Meeting Points Solution Method Considering Obstacles

In the research methodology of this paper, whether it is solving for a single meeting point or a meeting point within a specific subgroup of multiple meeting points, we utilize the principle of the Fermat point to determine an initial meeting point m_0 to narrow the search space and then quickly locate the final meeting point m through a grid search in the neighborhood of m_0. We refer to this method as the improved Fermat point method. The core idea of the Fermat point principle is to find a point that minimizes the sum of the distances to N known coordinate points; this point is the Fermat point, as shown in Equation (6):

$$min\sum d = \sum_{i=1}^{N} \sqrt{(x_0 - x_i)^2 + (y_0 - y_i)^2} \quad (6)$$

As shown in Figure 6, to obtain the meeting point m with the shortest total path length, we first input all relevant task coordinate points and quickly calculate an initial reference task intersection point m_0 using the Fermat point method. Subsequently, we invoke the underlying path-planning algorithm to plan the paths from all involved task coordinate points to m_0 and calculate the total length of these paths, denoted as $Length_0$, which serves as the reference path length value. Then, we further plan the paths from these task coordinate points to all neighboring grid cells v_i of m_0 and compute the corresponding total path length $Length_{vi}$. As shown in Equation (7), if $Length_{vi} \leq Length_0$, we set $m_0 = v_i$ and $Length_0 = Length_{vi}$. This process is repeated until all $Length_{vi} > Length_0$, at which

point we set $m = m_0$. Ultimately, we utilize the improved Fermat point method to obtain the task-meeting point m with the shortest total path length.

$$m_0 = \begin{array}{l} v_i \quad \exists\ Length_{vi} \leq \\ Length_0\ m_0 \quad \forall \\ Length_{vi} > Length_0 \end{array} \tag{7}$$

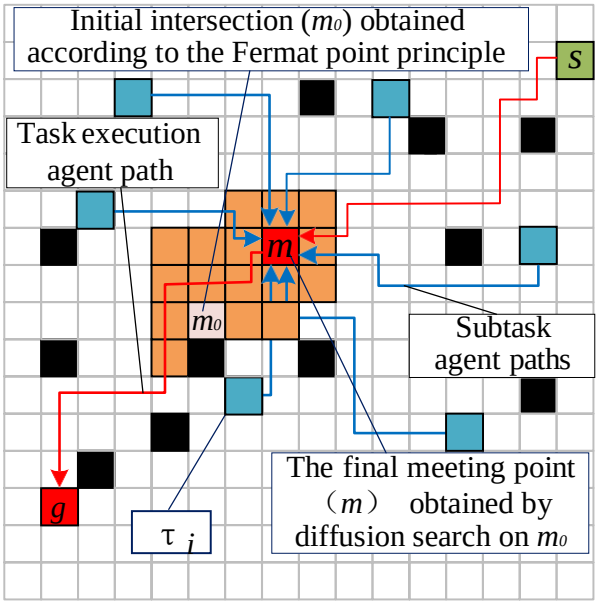

Figure 6. Improved Fermat point method for obtaining single or specific subgroup meeting points.

The solution may involve determining multiple meeting points in collaboration with multiple meeting points. In this case, we implement different strategies based on the number of agents within the cooperative group. When the number of agents in a single cooperative group $n = 2$ and the number of meeting points $N_m = 1$, then the determination of the meeting point is similar to that shown in Figure 6, using the improved Fermat point method directly. However, when the number of collaborative agents in a single group $n > 2$, the number of convergence points $N_m \in [1, n-1]$ and the number of agents in a single collaborative group n is determined by a combination of factors such as the task size, the scenario, and the map size. We need to follow these steps to solve multiple meeting points:

(1) First, we collect the position information of each sub-task starting point τ_i, the starting point s of the execution agent, and the task destination point g.

(2) Next, we connect the starting point s of the execution agent and the task destination point g to form the line segment L_{sg}. Then, we calculate the foot of the perpendicular from each sub-task starting point τ_i to the line segment L_{sg}, denoted as f_{ci}. As shown in Equation (8), based on the relative position of the horizontal coordinate of the foot of the perpendicular f_{ci} to the line segment L_{sg}, we divide the corresponding sub-tasks into three parts: pre-segment, intra-segment, and post-segment. In Equation (8), d_{sf} is the distance between point s and point f. Notably, in the particular case where the line segment L_{sg} is vertical, the division into three parts is based on the relative position of the vertical coordinate of the foot of the perpendicular f_{ci} to the line segment L_{sg}.

$$T_{part} = \begin{cases} 1 & d_{sf} + d_{gf} \neq d_{sg} \text{ and } d_{sf} < d_{gf} \\ 2 & d_{sf} + d_{gf} \neq d_{sg} \text{ and } d_{sf} > d_{gf} \\ 3 & d_{sf} + d_{gf} < d_{sg} \text{ and } d_{sf} > d_{gf} \end{cases} \quad (8)$$

(3) For sub-task points of the pre-segment, we input their coordinates together with the starting point s of the execution agent and use the improved Fermat point method to solve for the nearest meeting point p_s, as shown in the green box on the left side of Figure 7.

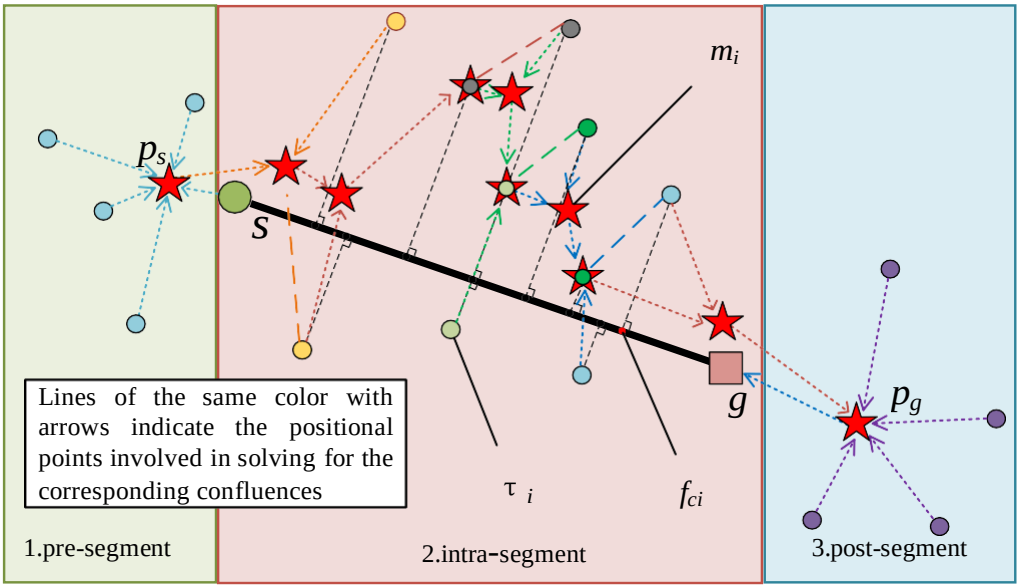

Figure 7. Schematic diagram of solving multiple meeting points within a collaborative group.

(4) For the sub-task points of the post-segment, we input their coordinates together with the task destination point g and utilize the improved Fermat point method to solve for the nearest meeting point p_g to these points, as illustrated in the blue box on the right side of Figure 7.

(5) The process for determining the meeting points of the intra-segment is relatively complex. First, we sort the horizontal coordinates of the feet of the perpendiculars cor- responding to the sub-task points (τ_{0i}) within the segment in ascending order using the bubble sort algorithm, ensuring that the feet closer to point s are ranked higher. This gives us an initial priority order for the agents within the segment. Subsequently, we adjust the starting order of the sub-task agents according to this priority order to accurately determine the meeting points in subsequent calculations.

(6) After ordering adjustment, the sub-task points need to be paired into q subgroups. As shown in Equation (9), if the number of sub-task points ($N_{\tau 0}$) is odd, and a post-segment meeting point p_g exists, we place the last sub-task points $\tau 0k$ and p_g into the last subgroup (SG_q). If p_g does not exist, we place $\tau 0k$ and the task destination point g into a subgroup.

$$SG_q = \begin{cases} \tau 0k, p_g \} & N_\tau 0 /2 = 1 \text{ and } p_g \textit{ Exist} = \textit{True} \\ \{\tau_{0k}, g\} & N_\tau 0 /2 = 1 \text{ and } p_g \textit{ Exist} = \textit{False} \end{cases} \quad (9)$$

(7) After sequencing adjustment, the first sub-task point in the ith subgroup within the same time segment is denoted as τ_{i1}. As shown in Figure 8, we use p_s or s (if p_s does not exist) to determine the first meeting point m_{11} of the first subgroup within the segment. Then, using m_{11}, τ_{11}, and τ_{12}, we calculate the second meeting point m_{12} of this subgroup. Following the same principle, we compute the two meeting points m_{i1} and m_{i2} for each remaining subgroup within the segment. If the second coordinate of the last subgroup is p_g or g, then the meeting point is $m_{q2} = p_g$ or $m_{q2} = g$, respectively. Otherwise, m_{q2} is calculated using p_g or g (if p_g does not exist) along with τ_{q1} and τ_{q2}. Finally, all the computed meeting points within the segment are stored in the meeting point list $Task_L$.

(8) After solving all subgroup meeting points, if p_s and p_g exist, they are inserted at the beginning and end of $Task_L$, respectively. Subsequently, the task goal point g is added to the end of $Task_L$. Finally, the ith meeting point in $Task_L$ is defined as m_i, which is used in subsequent segmented path planning.

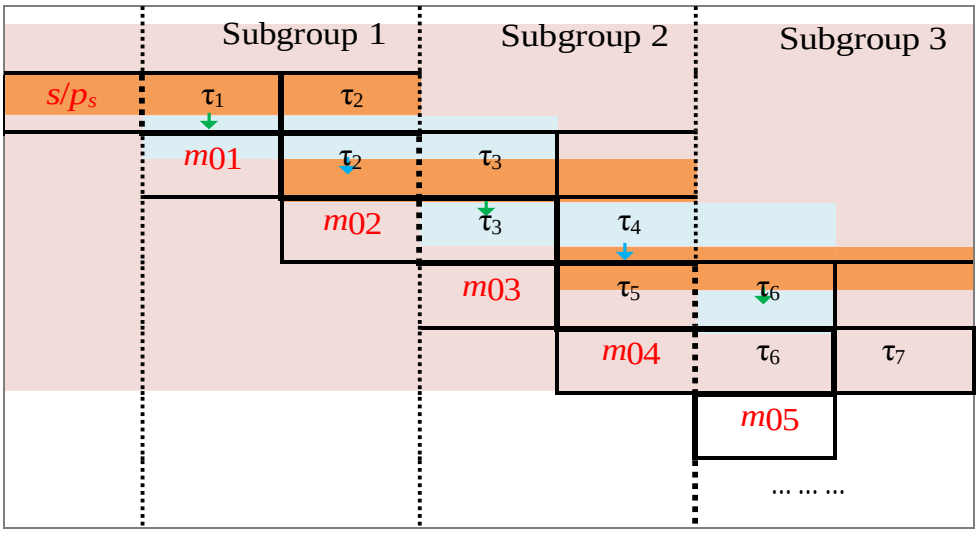

Figure 8. Schematic diagram of the meeting points of subgroups solved within the segment (Squares of the same color indicate the three coordinate points that need to be involved in solving a conflu- ence mi).

Several vital points need to be explained here: First, during the solving process for the meeting points, we do not directly involve the starting point s_i of the sub-task agent, as the path from s_i to the sub-task starting point τ_i can be planned directly and independently of the meeting points. Second, the pre-segment, intra-segment, and post- segment categorization of sub-task points, along with the priority adjustment of intra- segment sub-task points, ensures that the task-executing agent can perform task handovers with sub-task agents from nearby to far, minimizing redundant paths. Finally, as depicted in Figures 8 and 9, each subgroup is designed with two meeting points, and the meeting points of the preceding subgroup directly participate in the calculations of the subsequent subgroup, enhancing interconnectivity, shortening path lengths, and improving efficiency and performance.

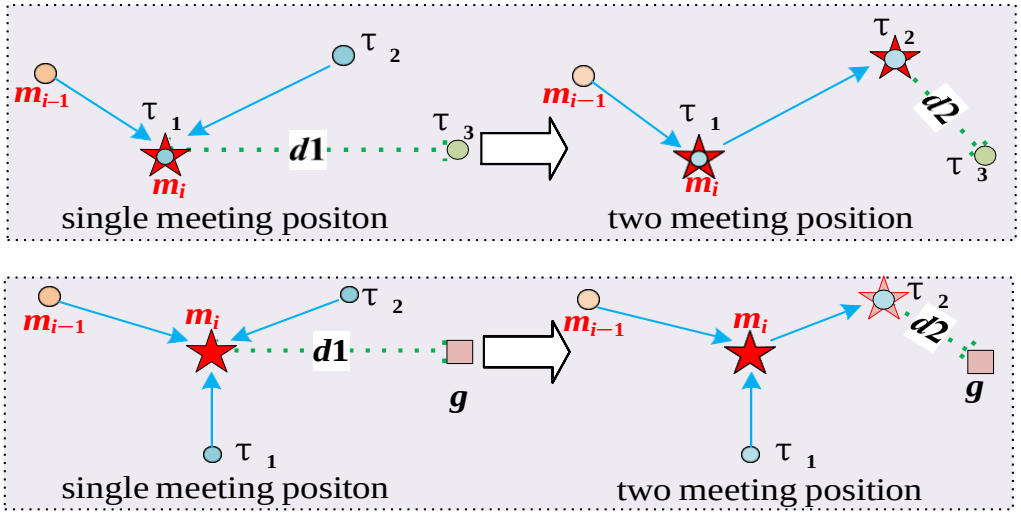

Figure 9. Comparison of task handover within a subgroup at one or two merging locations (Lines of the same color with arrows indicate the positional points involved in solving for the correspond- ing confluences).

3.1. Segmented Path Planning Strategy

As illustrated in Figure 10, to ensure that each group of collaborative agents efficiently and accurately completes task handovers at their respective meeting points, we implement segmented path-planning strategies explicitly tailored for sub-task agents and task execu- tion agents in terms of setting and planning goal points in the following way. During the prioritization process of planning collaborative task handover paths for sub-task agents, once a sub-task agent reaches its initial goal point (i.e., the starting point of the sub-task,

τ_i), its goal point is immediately updated to the corresponding final goal point (i.e., the meeting point, m_i).

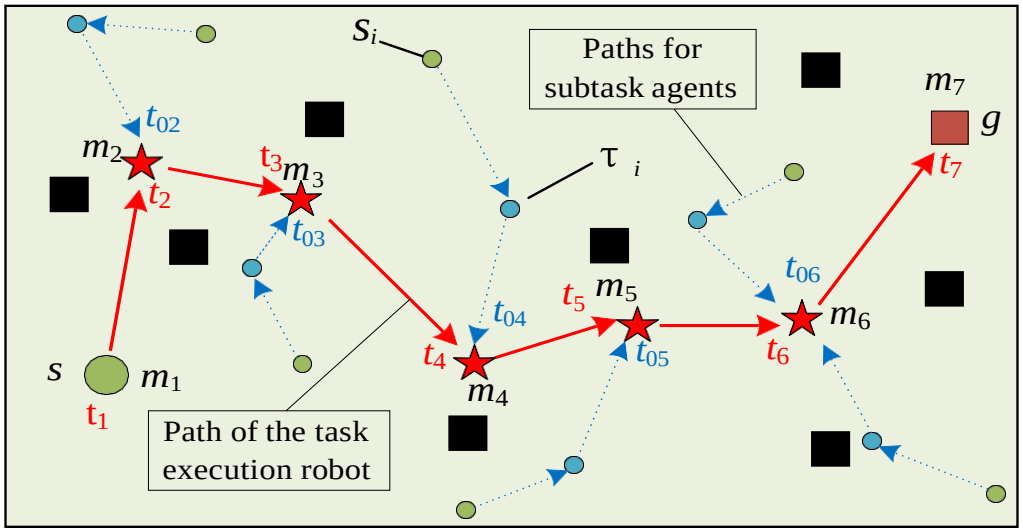

Figure 10. Schematic diagram of segmented path planning for a collaborative task handover agent.

After completing the segmented path planning for each sub-task agent within the collaborative group, it is necessary to compile the arrival time t_{0i} (Equation (10)) of the last agent to reach each meeting point, which will then be utilized in the planning process for the task execution agent.

$$t_{oi} = \max^{n} \sum^{N} \tau 0 \ \pi_i, \tag{10}$$

The complexity of planning collaborative task handover paths for the task execution agent escalates due to the interplay of multiple meeting points. To ensure a smooth transition of tasks, we must factor in the latest arrival time t_{0i} recorded in (1) for sub-task agents at their respective meeting points. As the task execution agent plans routes to these meeting points m_i, it compares its estimated arrival time t_i with t_{0i}. As shown in Equation (11), if t_i is greater than or equal to t_{0i}, indicating that all sub-task agents have arrived, the task execution agent will wait for one time step to facilitate the task handover with the arrived sub-task agents, followed by replacing its goal point. Conversely, if t_i is less than t_{0i}, signifying that the task execution agent has reached the meeting point ahead of the sub-task agents, it will execute a waiting operation until t_i equals $t_{0i}+1$ before proceeding with the goal point replacement.

$$t^{wait} = \begin{cases} 1 & t_i \geq t_{0i} \\ t_i - t_{0i} + 1 & t_i < t_{0i} \end{cases} \tag{11}$$

By adopting this clear and well-defined segmented path planning strategy, we ensure the orderliness and efficiency of the collaborative agents during task execution, thereby minimizing confusion and delays in the task handover process.

3.2. Hybrid Solution Mode Switching Mechanism

When utilizing a collaborative path planning approach with multiple meeting points, while it can offer optimization in path length, in certain specific scenarios, the numerous and dispersed handover points within the movement-constrained areas of the map can make it exceedingly challenging, if not impossible, to identify and reach these meeting points, potentially leading to solution failure. In such cases, the more straightforward and more direct approach of solving for a single meeting point may paradoxically have a greater chance of successfully finding a solution. Consequently, this paper proposes an intelligent switching strategy that integrates both the multi-meeting-point and single- meeting-point solving modes. The aim is to prioritize ensuring the algorithm's success

rate while also optimizing the path length. As depicted in Equation (12) and Figure 11, the algorithm initially attempts to solve problems using the multi-meeting-point solving mode (*MMP*). If the solving time in this mode $t \geq 1/6 \cdot T_0$ and the number of solving failures in the multi-meeting-point solving mode $c \geq 1$, the algorithm automatically switches to the single-meeting-point solving mode (*SMP*). Even in this simplified mode, if the solution remains elusive, the algorithm continues to seek a solution by adjusting the group priorities. The solution complexity is higher in the multi-meeting-point solving model because a collaborative group needs to solve for multiple meeting locations. In contrast, a collaborative group only needs to solve for one meeting location in the single-meeting-point solving model, which has a lower solution complexity in comparison. However, the path solution obtained by all agents performing task handover at a single meeting point produces redundant paths that are longer and consume more energy to move than performing task handover at multiple meeting points. Therefore, the multi-meeting-point solving model is preferred for solving when conditions allow one to obtain a better path scheme.

$$MD = \begin{matrix} MMP & t < 1/6 \cdot T_0 \text{ or } c < 1 \\ SMP & t \geq 1/6 \cdot T_0 \text{ and } c \geq 1 \end{matrix} \quad (12)$$

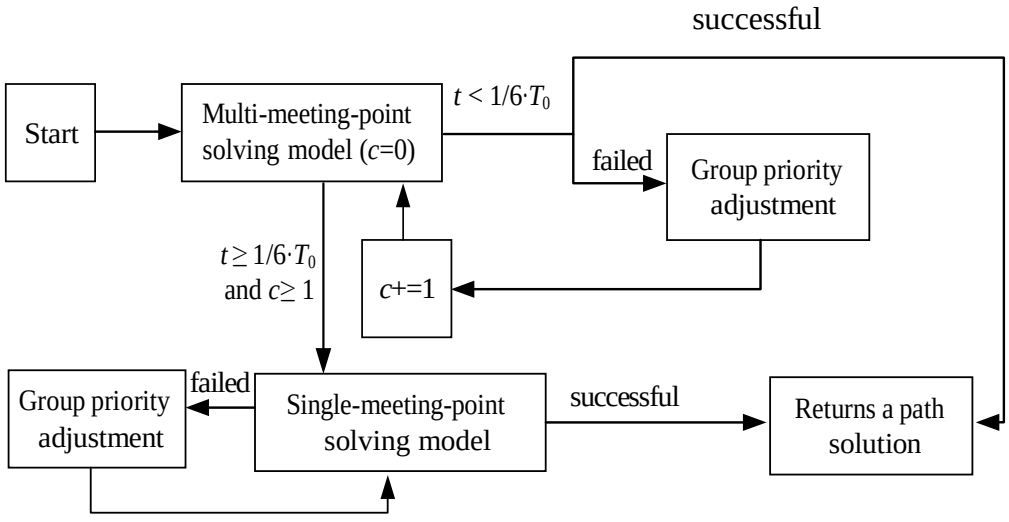

Figure 11. Schematic diagram of switching between multi-meeting-point and single-meeting-point solving modes.

In addition, two prioritization methods are used in this paper to obtain better optimal solutions and higher success rates. In the multi-meeting-point solving mode, the algorithm performs priority adjustments within individual collaborative groups to ensure the task execution agent can hand over tasks with sub-task agents in an optimal sequence, thereby reducing unnecessary path redundancy. For the entire multi-agent system, priority ad- justments focus on the entire group, aiming to enhance the success rate of the solution by optimizing interactions between groups. The group prioritization adjustment method is shown in Equation (13), where P_{Gi} is the group priority of $group_i$ and P_{GF} is the priority of the group where the solution failed:

$$P_{Gi} = \begin{cases} 1 & P_{Gi} = \\ P_{GF}\, i+1 & P_{Gi} \\ & < P_{GF} \\ i & P_{Gi} > \\ & P_{GF} \end{cases} \tag{13}$$

3.3. Pseudocode and Flowchart of the Co-DPSIPP$_{ms}$ Algorithm

The pseudocodes for the Co-DPSIPP$_{ms}$ algorithm are presented in Algorithms 1 and 2. Algorithm 1 is the planning system's upper layer and is responsible for priority adjustments, solving mode switching, and safety interval updates. Algorithm 2, conversely, constitutes

the lower layer of the planning system, tasked with segmenting and planning collision-free paths for individual agents.

Algorithm 1: Co-DPSIPP$_{ms}$ algorithm

---

input: $Group = \{\ldots, group_i = (agents_a, agent_b, task_i), \ldots\}$, Map, $T0$, $MD = MMP$

%$MD = MMP$, initial use of multi-meeting-point solving mode

output: *Paths*, *length*

1: **while** $t < T_0$ **do**

2: **for** $group_i$ in *Group* **do**

3: **if** $MD{=}MMP$ **then**

4: $newGoal \leftarrow Mi1 \leftarrow$CalMultipleMeetingPoints($group_i$)

%Solving for multiple meeting points

5: **end if**

6: **if** $MD = SMP$ **then**

7: $newGoal \leftarrow Mi2 \leftarrow$CalSingleMeetingPoint($group_i$)

%Solving for single meeting point

8: **end if**

9: **for** agent in $group_i$ **do**

10: $res, \ path_i \leftarrow$iSIPP(*agent*, *id*, *Map*, *newGoal*)

11: **if** $res = success\,ful$ **then**

12: $path_i$ insert *Paths*, update $Safe Interval$

%Update safe intervals to avoid future conflicts

13: **end if**

14: **if** $res = failed$ **then**

15: **if** $MD = MMP$ and $t \geq 1/6 \cdot T_0$ **then**

16: $MD = MSP$

17: **end if**

18: $newGroup \leftarrow$DeterReScheduling($group_i$, *Group*)

%Set the priority of failed groups to the highest

19: $Group \leftarrow newGroup$

20: $Paths \leftarrow \emptyset, Safe\_interval \leftarrow InitialSafeInterval$

21: **end if**

22: **end for**

23: **end for**

24: **return** *Paths, length*

25: **end while**

26: **return** , ∅ , 0

Algorithm 2: iSIPP algorithm

---

input: *agent, id, Map, newGoal,Replaced=False*

output: pat*h*

1: **while** *curNode* /= *agentGoal* **do**

2: expand nodes

using A* 3: **if** OPEN

= ∅ **then**

4: **return** *failed*, ∅

5: **end if**

6: **if** not *Replaced* **then**

7: **if** *curNode = agentGoal* **then**

8: **if** *agent* is $agent_b$ **then**

9: Perform the wait operation according to Equation (11)

10: **end if**

11: $agentGoal = newGoal_{id}$

%A unvisited meeting location as new

goal point 12: **if** $newGoal_{id}$ is *agentFinalGoal*

then

13: *Replaced = True* %Plan to the ultimate goal

Algorithm 2: iSIPP algorithm

14: **end if**
15: **end if**
16: **end if**
17: **if** *Replaced* **then**
18: **if** *curNode* = *agentGoal* **then**
19: **return** *success f ul*, *path*
20: **end if**
21: **end if**
22: **end while**

Figure 12 details the complete flow of the Co-DPSIPP$_{ms}$ algorithm, which comprises six crucial components: meeting point solving, segmented path planning, global safety interval updating, switching between multi-meeting-point and single-meeting-point solving modes, and group priority adjustments. These components work in concert to ensure that the algorithm can optimize the path length and efficiency of task execution while guaranteeing a high success rate of the solution.

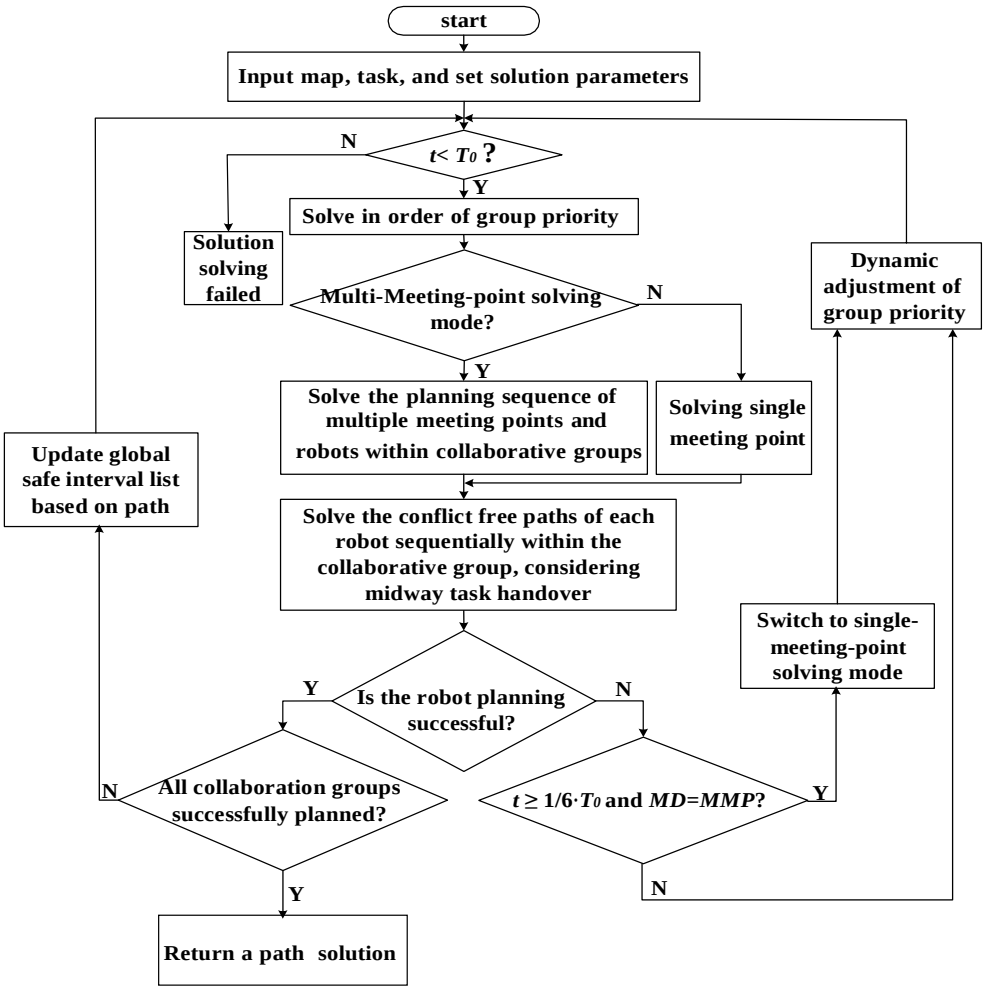

Figure 12. Flow chart of the Co-DPSIPP$_{ms}$ algorithm.

In the Co-DPSIPP$_{ms}$ algorithm, the majority of the computation time is focused on solving for the meeting points. When N_{group} collaborative groups are operating simulta- neously, with each group containing n agents and each group requiring k meeting points for task handovers, the solution for each meeting point involves r iterations of the search. Under this scenario, the underlying single-agent path planning algorithm will be invoked

$k \cdot r \cdot n \cdot N_{group}$ times during the process of solving for the meeting points. As a result, the time complexity of solving all meeting points can be expressed as follows:

$$O(Time) = k \cdot r \cdot N_{group} \sum_{i=0}^{n} O(b)^{Ti} \quad (14)$$

In Equation (14), b represents the number of states that the algorithm can expand outward during the node expansion process, T_i denotes the length of the path for a single agent (as a measure of path search complexity), and $\sum_{i=0}^{n} O(b)^{Ti}$ represents the time complexity of formally planning the path once all goal points are known. Due to the need to repeatedly invoke the underlying path planning algorithm while solving for meeting points, the time complexity of this part is almost $k \cdot r \cdot N_{group}$ times that of formally planning the path. These data show a significant increase in the computational complexity of the Collaborative Multi-Agent Path Finding problem (Co-MAPF) compared to the classical MAPF problem. This increase is primarily attributed to the additional computations and iterative searches introduced by solving for meeting points.

4. Simulation Experimental Analysis

4.1. Experimental Parameter Settings

This paper compares the performances of the different collaborative agent path- planning algorithms through three simulation experiments. Simulation Experiment 1 primarily focuses on the performance of the Co-CBS algorithm and the Co-DPSIPP$_{ms}$ algorithm in scenarios where only two agents collaborate. Simulation Experiment 2 pro- vides a more comprehensive evaluation of three algorithms: Cooperative Dynamic Priority SIPP with a single meeting point (Co-DPSIPP$_s$), Cooperative Dynamic Priority SIPP with multiple meeting points (Co-DPSIPP$_m$), and Cooperative Dynamic Priority SIPP with multi-meeting-point and single-meeting-point solving mode switching (Co-DPSIPP$_{ms}$). Additionally, Simulation Experiment 3 exemplifies the impact of the number of agents within a single collaborative group on the solution results of both the Co-DPSIPP$_s$ and Co-DPSIPP$_{ms}$ algorithms.

The experiments were conducted on a Windows 10 PC with an Intel Core i7 (3.6 GHz) CPU and 32 GB of RAM, and the algorithms ran on an Ubuntu 20.04 environment installed on a VMware17 virtual machine to ensure a fair comparison on a unified platform. In order to evaluate the algorithm's solution efficiency, we set each planning limit time T_0 to 5 min. If an algorithm failed

to return a valid solution within this time, the corresponding instance was considered a failure.

The experimental maps included standard Nest, Empty, Maze, and Warehouse maps, as shown in Figure 13, simulating environments of varying complexity. For experiments involving *n* agents within a single collaborative task, we utilized the *n* sets of coordinates from the instance files (i.e., Scenarios files) accompanying the standard maps to set the starting positions of the agents, sub-task starting points, and task goal points. The starting point and goal point of the first sub-task correspond to the starting and goal points of the first set of coordinates, the starting point of the first sub-task agent and the starting point of the task execution agent correspond to the starting and goal points of the second set of coordinates, and the starting points of the remaining *n*-2 sub-task agents and sub- task starting points correspond to the starting and goal points of the remaining *n*-2 sets of coordinates.

In Simulation Experiment 1, we set the number of agents within a single collaborative group to $n = 2$. We gradually increased the number of collaborative task groups N_{group} from 6 to 30 to evaluate the performance of the algorithms under different collaboration group sizes. In Simulation Experiment 2, we fixed the number of agents within a single collaborative group to $n = 10$. We incrementally increased the number of collaborative task groups N_{group} from 1 to 5 to analyze the performance of the algorithms in multi-group collaboration scenarios. To further explore the impact of the number of agents within a

single collaborative group on the experimental results, we conducted an additional set of experiments where N_{group}=1, and the number of agents within a single collaborative group *n* was gradually increased from 5 to 25. Each experiment was repeated 5 times, with each test comprising 25 instances, to ensure the reliability and stability of the results. The *runtime* metric represents the time the algorithm takes to return a valid solution during the solution process, reflecting the algorithm's solution efficiency. When comparing *runtime*, total path length (*length*), and total path cost (*f lowtime*), we took the average values of public solutions as the basis for comparison to more accurately assess the merits of the algorithms. Additionally, we bolded the best-performing data among several algorithms for a more intuitive comparison.

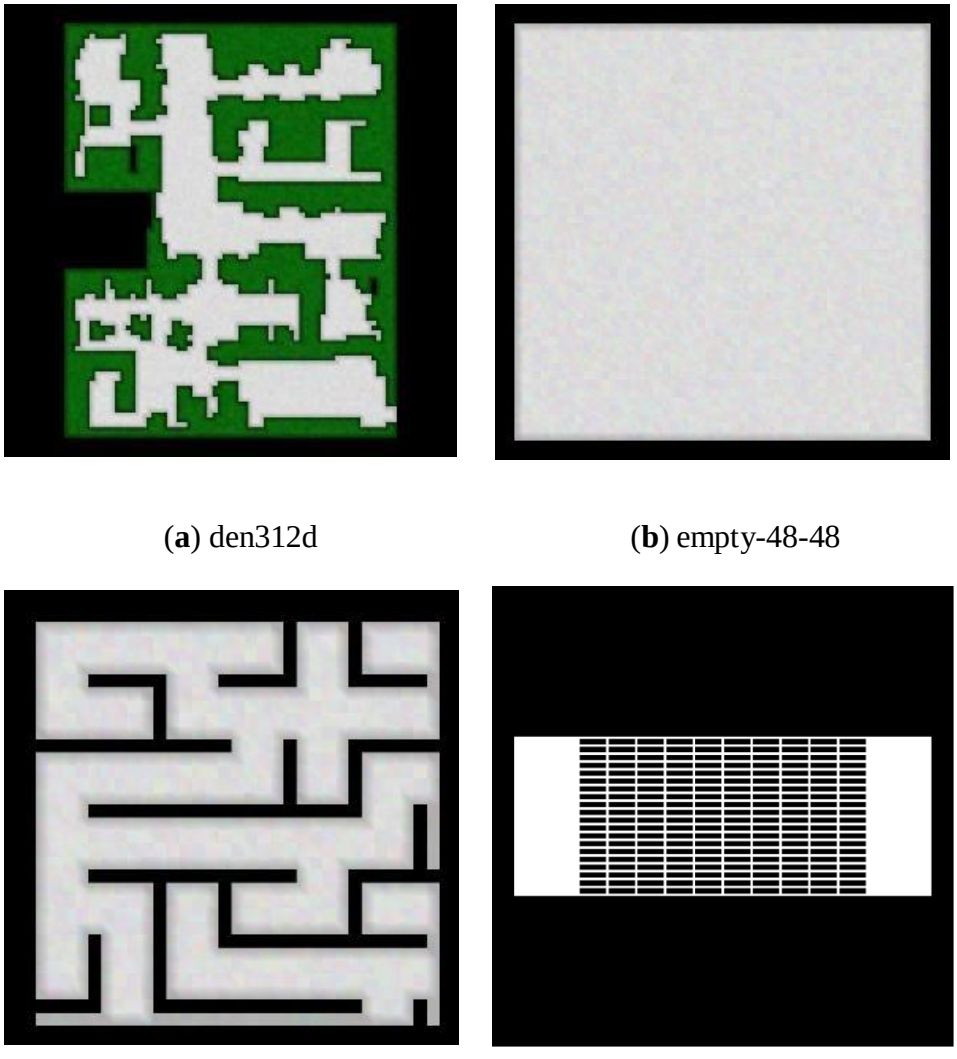

(**a**) den312d (**b**) empty-48-48

(**c**) maze-32-32-4 (**d**) warehouse-10-20-10-2-1

Figure 13. Nest, Empty, Maze, and Warehouse benchmark maps.

In Figure 14, we present the multi-agent path planning algorithm's planned paths utilizing multiple and single-meeting-point collaboration

formats, and a line of one color denotes a robot's path. Figure 14a,b corresponds to these two collaboration formats, respectively, involving 9 sub-task agents and 1 task execution agent working together to complete tasks. In the figures, the green circles represent the starting points of the task execution agent, the red rectangles mark the task goal points, and the red five-pointed stars indicate the meeting points calculated by the algorithm. It is evident from the figures that the path in the single meeting-point-collaboration format tends to converge toward a single handover point, leading to longer redundant segments in the path. In contrast, the path in the multi-meeting-point collaboration format allows for task handovers at multiple different handover points, enabling more flexible path planning and significantly reducing the length of redundant paths. This optimization not only improves the overall

task execution efficiency but also decreases the energy consumption of agents during task execution.

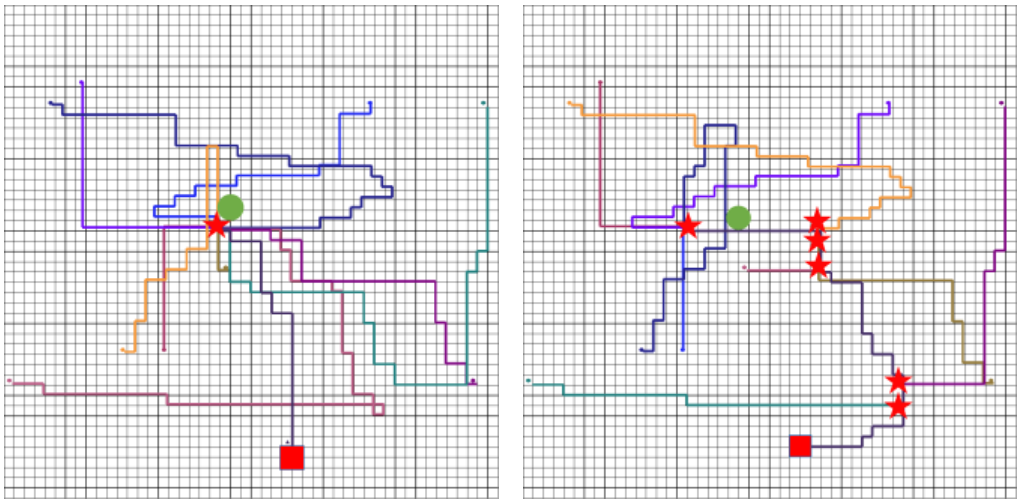

(**a**) Single meeting point (9-to-1) (**b**) Multiple meeting points (9-to-1)

Figure 14. Path diagram of a single group collaborative task (*n* = 10).

4.2. Simulation Experiment 1

Figure 15 and Table 1 present a comparative analysis of the test results between the Co-CBS algorithm and the Co-DPSIPP$_{ms}$ algorithm when only two agents collaborate. In the 1-to-1 collaboration scenario, as depicted in Figure 15, the Co-DPSIPP$_{ms}$ algorithm demonstrates significant advantages over the Co-CBS algorithm, particularly regarding the solution success rate. Specifically, across four different maps (Nest, Empty, Maze, and Warehouse), the solution success rate of Co-DPSIPP$_{ms}$ improved by 60%, 53.6%, 19.2%, and 24%, respectively, showing remarkable superiority. Furthermore, by comparing the maximum number of solvable collaboration task groups between the two algorithms, we found that Co-DPSIPP$_{ms}$ was able to solve more collaboration task groups on all four maps. Notably, on the Nest and Maze maps, the number of solvable collaboration task groups achieved by Co-DPSIPP$_{ms}$ was more than twice that by Co-CBS. In summary, the Co-DPSIPP$_{ms}$ algorithm boasts a higher solution success rate and handles more collaboration task groups and agent instances on these four maps, demonstrating more robust solving capabilities and adaptability.

Table 1. Comparison of path solutions between Co-CBS and Co-DPSIPP$_{ms}$ algorithms in 1-to-1 collaboration.

Map	N_{group}	*Length*/Step		*Flowtime*/Step		*Runtime*/s	
		Co-DPSIPP$_{ms}$	Co-CBS	Co-DPSIPP$_{ms}$	Co-CBS	Co-DPSIPP$_{ms}$	Co-CBS
den312d	6	**768.8**	893.9	1014.2	**972.7**	**16.12**	43.42
empty-48-48	6	**467.88**	536.12	665.52	**592**	**4.63**	8.47
	12	**950.72**	1089.94	1253.72	**1194.44**	**17.68**	22.29
	18	**1426.6**	1607.8	1912.2	**1777.2**	**54.29**	128.65
maze-32-32-4	6	**620.75**	636.25	786.5	**729.75**	**28.91**	46.89
warehouse-10-20-10-2-1	6	**1254.4**	1396.93	1630.86	**1540.2**	**10.34**	70.71
	12	**2379.33**	2598.33	3096	**2847.33**	**26.38**	156.83

Note: The data marked in bold are the best performing data from the results of the comparison algorithm.

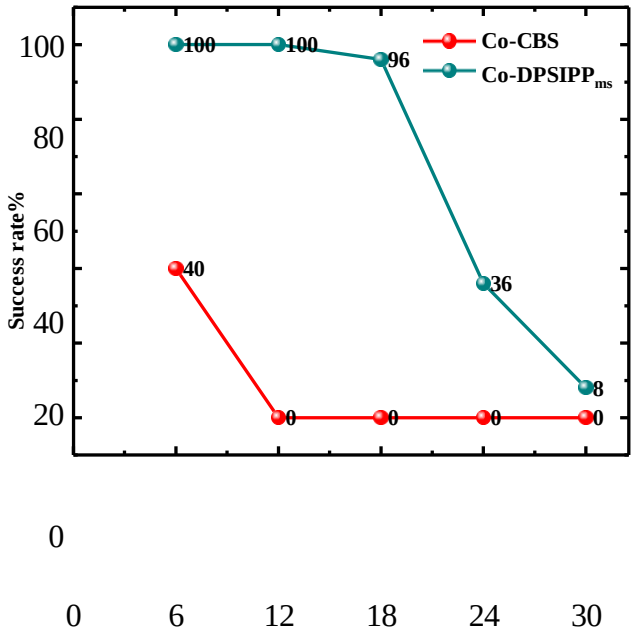

(**a**) den312d

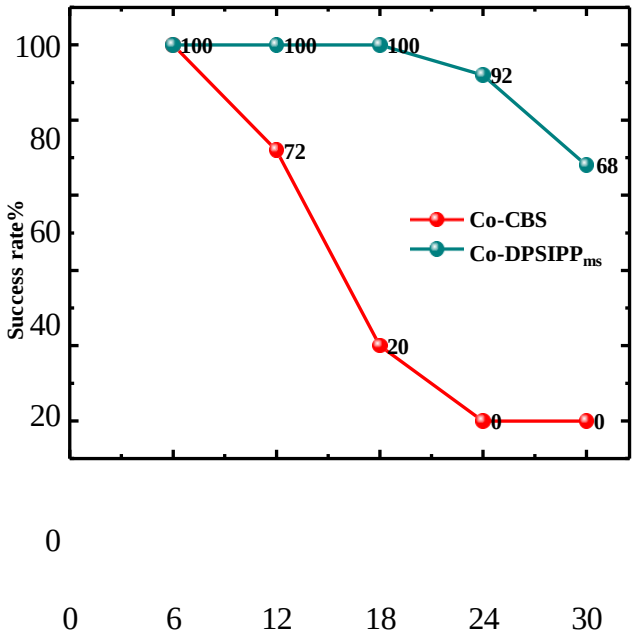

(**b**) empty-48-48

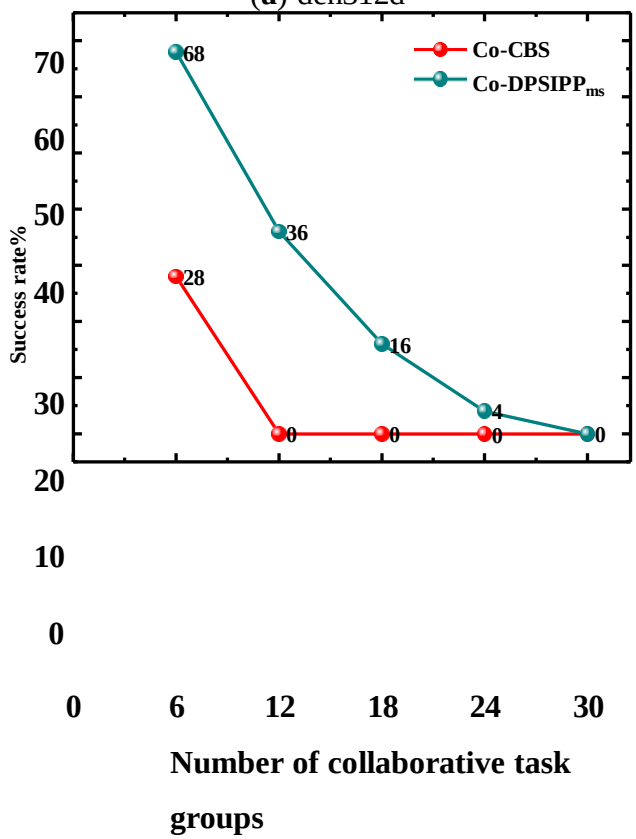

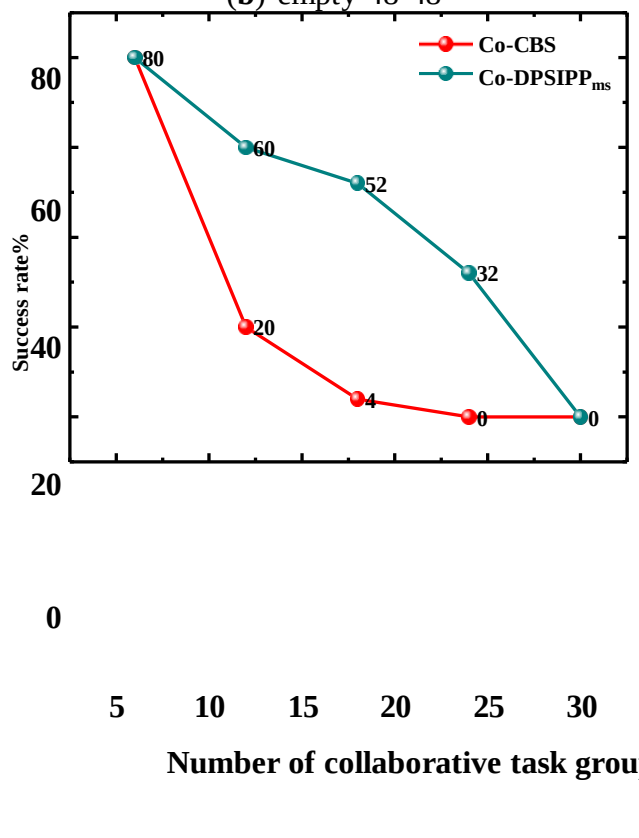

(**c**) maze-32-32-4 (**d**) warehouse-10-20-10-2-1

Figure 15. The success rates of the Co-CBS and Co-DPSIPP$_{ms}$ algorithms in the 1-to-1 collaboration.

Table 1 reveals that the Co-DPSIPP$_{ms}$ algorithm exhibits significant advantages over the Co-CBS algorithm regarding the total path length and algorithm solving time. Specif- ically, on the Nest, Empty, Maze, and Warehouse maps, the path solutions generated by Co-DPSIPP$_{ms}$ are 13.9%, 12.2%, 2.4%, and 9.3% shorter in total path length, respectively, than those generated by Co-CBS. Concurrently, the solving times are reduced by 62.8%, 41.3%, 38.3%, and 84.2%, respectively. These results imply that the Co-DPSIPP$_{ms}$ algo- rithm can find path solutions in a much shorter time in addition to maze maps, and the obtained path solutions are able to reduce energy consumption by about 10% compared to the Co-CBS algorithm, which is an essential economic and environmental benefit in practical applications.

However, regarding the total path cost, the Co-DPSIPP$_{ms}$ algorithm is inferior to the Co-CBS algorithm. This is primarily due to the optimization objective of the Co-DPSIPP$_{ms}$ algorithm, which focuses on minimizing the total path length. In some scenarios, to avoid unnecessary energy consumption, the task execution agent may need to wait at the meeting point for the sub-task agents to arrive for task handover, resulting in a higher path cost than the Co-CBS algorithm. Nevertheless, considering the significant advantages of the Co-DPSIPP$_{ms}$ algorithm in terms of path length and solving time, it holds a high application value and potential in multi-agent cooperative path planning.

Table 2. Path solution comparison of the Co-DPSIPPs and Co-DPSIPPms algorithms in the 9-to-1 collaboration.

Map	***Ngroup***	***Length*/Step**		***Flowtime*/Step**		***Runtim***	
		Co-DPSIPP$_{ms}$	**Co-DPSIPP$_{s}$**	**Co-DPSIPP$_{ms}$**	**Co-DPSIPP$_{s}$**	**Co-DPSIPP$_{ms}$**	**Co-DPSIPP$_{m}$**
den312d	1	**760.38**	806	**852.84**	929	21.18	**7.86**
	2	**1433.6**	1638.6	**1594.4**	1860.6	121.37	**73.37**
	3	**2262**	2446	**2567.5**	2765.5	157.45	**103.88**
	4	**2702**	3307.5	**2920.25**	3793.25	233.2	**283.64**
	5	**3190**	4083	**3433**	4613	241.32	**300**
empty-48-48	1	**454.25**	495.85	**506.15**	565.85	2.64	**3.05**
	2	**855.66**	1014.44	**922.16**	1153.33	35.71	**26.92**
	3	**1253.53**	1537.33	**1363.6**	1757.93	39.85	**84.91**
	4	**1653**	2076.63	**1770.63**	2356.81	116.41	**213.75**
	5	**2108.1**	2607.44	**2284.67**	2951.22	213.45	**293.93**
maze-32-32-4	1	**604.9**	637.7	**727**	757.8	19.76	**8.92**
	2	**1213.75**	1404.87	**1427**	1695.87	42.35	**25.61**
	3	**1797.5**	2087.5	**2152.5**	2631.5	80.04	**50.82**
	4	**2612.66**	2808	**3475.66**	3812	149.02	**92.46**
warehouse-10-20-10-2-1	1	**951.3**	1113.95	**1035.08**	1268.91	7.94	**4.49**
	2	**2185.68**	2526.36	**2373.89**	2860.26	65.34	**74.71**
	3	**3689.61**	3813.53	**4154.53**	4295.53	131.82	**118.85**
	4	**5373.2**	5523.2	**5984**	6185.4	212.97	**167.66**
	5	**6632.66**	7100.66	**7451**	7969	259.82	**229.61**

Note: The data marked in bold are the best performing data from the results of the comparison algorithm.

Furthermore, the data in Table 2 reinforce the superiority of the Co-DPSIPP$_{ms}$ algo- rithm in path planning. Regarding the average total path length, Co-DPSIPP$_{ms}$ achieves reductions of 13.14%, 16.34%, 10.5%, and 8.12% compared to Co-DPSIPP$_{s}$ across the four maps. This significant improvement is attributed to the ability of the Co-DPSIPP$_{ms}$ algo- rithm to guide the sub-task agents and task execution agents to select more suitable locations on the map for task handover, effectively reducing redundant paths. Co-DPSIPP$_{ms}$ not only decreases the energy consumption of the agentic system but also saves operational costs. The Co-DPSIPP$_{ms}$ algorithm also demonstrates a clear advantage regarding the average to- tal path cost, reducing the total cost by 15.52%, 20.04%, 11.68%, and 9.68% on the four maps, respectively. Regarding algorithm runtime, on the relatively spacious Nest and Empty maps, the Co-DPSIPP$_{ms}$ algorithm, which switches between multiple-meeting-point and single-meeting-point solving modes when $N_{group} > 3$, can return solutions faster. However, in complex and narrow maps, such as Maze and Warehouse, the Co-DPSIPP$_{s}$ algorithm with a single-meeting-point solving mode returns solutions more quickly.

From the above results, it is evident that the Co-DPSIPP$_{ms}$ algorithm performs ex- ceptionally well on the Nest, Empty, and Maze maps, while its advantage diminishes slightly on the Warehouse map with severely restricted mobility. Compared to Co-DPSIPP$_{s}$, Co-DPSIPP$_{ms}$ significantly improves the solution success rate, shortens the path length, and reduces the total path cost at the expense of a slightly longer algorithm runtime.

5.3. *Simulation Experiment 3*

To further investigate the impact of increasing the number of cooperative agents on the performance of the two algorithms, we conducted tests on an obstacle-free empty map, and the results are presented in Figure 17.

By comparing instances where both Co-DPSIPP$_{s}$ and Co-DPSIPP$_{ms}$ can find solutions in a single run, we observed that as the number of agents in a single cooperative group increases, the Co-DPSIPP$_{ms}$ algorithm, which employs multiple meeting points, exhibits increasingly significant optimization effects regarding path length and total path cost. This is because, as the number of agents in a single cooperative group increases, the single-

meeting-point approach is more prone to generating redundant paths. In contrast, the Co-DPSIPP$_{ms}$ algorithm effectively reduces these redundancies through the multi-meeting- point approach. However, when the number of agents reaches a certain threshold, the optimization effect tends to stabilize due to the influence of other agents' movements. This result indicates that within a certain range of the number of single-group cooperative agents, the Co-DPSIPP$_{ms}$ algorithm, which operates through the collaboration of multiple meeting points, can achieve a better path solution by sacrificing a certain amount of solution

5. Conclusions

Co-MAPF surpasses traditional MAPF in tackling tasks and significantly enhances system efficiency in most cases. In this paper, we innovatively propose a multi-robot path- planning algorithm to solve the problem of "many-to-one" collaborative robot tasks, which allows collaborative agents to perform task handovers at multiple meeting points. This advancement effectively mitigates the issue of excessively long redundant paths that occur during task handovers at a single meeting point. Furthermore, we incorporate an automatic switching strategy between multi-meeting-point and single-meeting-point solving modes to boost solution success rates. When the multi-meeting-point solving mode encounters difficulties, the algorithm seamlessly transitions to the single-meeting-point solving mode, ensuring a greater likelihood of successful solutions.

The simulation results unequivocally demonstrate the superiority of the proposed Cooperative Dynamic Priority Safe Interval Path Planning with multi-meeting-point and single-meeting-point solving mode switching (Co-DPSIPP$_{ms}$) algorithm. Compared to the Co-CBS algorithm, Co-DPSIPP$_{ms}$ achieves an average 39.20% increase in the solution success rate, a 9.45% reduction in total path length, and a 56.65% decrease in the solution time. Compared to Co-DPSIPP$_{s}$, the variant with a single meeting point, Co-DPSIPP$_{ms}$, exhibits a 15.4% improvement in the solution success rate, a 12.03% reduction in the total path length, and a 14.23% decrease in the total path cost. These findings indicate that the Co- DPSIPP$_{ms}$ algorithm significantly enhances solution success rates and shortens path lengths. Notably, as the number of agents within a specific range increases, the optimization effects on the total path length and cost become more pronounced, highlighting the scalability.

Efficiency of the proposed algorithm. Finally, the practicality and feasibility of the path planning solution devised by our algorithm are further validated through the actual execution results of CoCube agents.

In the future, we will focus on several core areas to deeply optimize algorithms, in- cluding enhancing algorithm execution efficiency, improving the quality of path planning solutions, achieving scientific and rational task allocation, and strengthening the collabora- tive working mechanism among multiple agents. Our goal is to realize more efficient and superior path-planning solutions.

References

1. Stern, R.; Sturtevant, N.; Felner, A.; Koenig, S.; Ma, H.; Walker, T.T.; Li, J.; Atzmon, D.; Cohen, L.; Satish Kumar, T.K.; et al. Multi- agent pathfinding: Definitions, variants, and benchmarks. In Proceedings of the International Symposium on Combinatorial Search, Napa, CA, USA, 16–17 July 2019; Volume 10, pp. 151–158.
2. Ren, Z.; Rathinam, S.; Choset, H. A conflict-based search framework for multiobjective multiagent path finding. *IEEE Trans. Autom. Sci. Eng.* **2022**, *20*, 1262–1274. [CrossRef]
3. Ali, Z.A.; Yakovlev, K. Safe Interval Path Planning with Kinodynamic Constraints. In Proceedings

of the AAAI Conference on Artificial Intelligence, Washington, DC, USA, 7–14 February 2023; Volume 37, pp. 12330–12337.

4. Cohen, L.; Wagner, G.; Chan, D.; Choset, H.; Sturtevant, N.; Koenig, S.; Satish Kumar, T.K. Rapid randomized restarts for multi-agent path finding solvers. In Proceedings of the International Symposium on Combinatorial Search, Stockholm, Sweden, 14–15 July 2018; Volume 9, pp. 148–152.
5. Lin, C.; Han, G.; Du, J.; Xu, T.; Lv, Z. Spatiotemporal congestion-aware path planning toward intelligent transportation systems in software-defined smart city IoT. *Internet Things J.* **2020**, *7*, 8012–8024. [CrossRef]
6. Yu, C.; Jia-Qiang, E.; Hao, Z.; Yuan-Wang, D. Driving-Record-Based Distributed Path-Planning for Autonomous Vehicle. In Proceedings of the International Conference on Intelligent Transportation, Big Data and Smart City, Xi'an, China, 19–20 December 2015; pp. 320–323.
7. Sun, N.; Shi, H.; Han, G.; Wang, B.; Shu, L. Dynamic path planning algorithms with load balancing based on data prediction for smart transportation systems. *IEEE Access* **2020**, *8*, 15907–15922. [CrossRef]
8. Fu, X.; Li, C.; Hui, Y.; Hui, Y.; Yang, J. Space-Time Map Based Path Planning solution in Large-Scale Intelligent Warehouse System. In Proceedings of the International Conference on Intelligent Transportation Systems, Rhodes, Greece, 20–23 September 2020; pp. 1–6.
9. Shi, Y.; Hu, B.; Huang, R. Task allocation and path planning of many robots with motion uncertainty in a warehouse environment. In Proceedings of the International Conference on Real-Time Computing and Robotics, Xining, China, 15–19 July 2021; pp. 776–781.
10. Chen, X.; Li, Y.; Liu, L. A coordinated path planning algorithm for multi-robot in intelligent warehouse. In Proceedings of the International Conference on Robotics and Biomimetics, Dali, China, 6–8 December 2019; pp. 2945–2950.
11. Wen, H.; Lin, Y.; Wu, J.B. Co-evolutionary optimization algorithm based on the future traffic environment for emergency rescue path planning. *IEEE Access* **2020**, *8*, 148125–148135. [CrossRef]
12. Dresner, K.; Stone, P. A multiagent approach to autonomous handover point management. *J. Artif. Intell. Res.* **2008**, *31*, 591–656. [CrossRef]
13. Le, C.; Pham, H.X.; La, H.M. A Multi-Robotic System for Environmental Cleaning. *arXiv* **2018**, arXiv:1811.00690.
14. Phillips, M.; Likhachev, M. Sipp: Safe interval path planning for dynamic environments. In Proceedings of the 2011 IEEE International Conference on Robotics and Automation, Shanghai, China, 9–13 May 2011; pp. 5628–5635.
15. Silver, D. Cooperative pathfinding. In Proceedings of the AAAI Conference on Artificial

Intelligence and Interactive Digital Entertainment, Marina Del Rey, CA, USA, 1–3 June 2005; Volume 1, pp. 117–122.

16. Sharon, G.; Stern, R.; Felner, A.; Sturtevant, N.R. Conflict-based search for optimal multi-agent pathfinding. *Artif. Intell.* **2015**, *219*, 40–66. [CrossRef]
17. Wagner, G.; Choset, H. M*: A complete multirobot path planning algorithm with performance bounds. In Proceedings of the International Conference on Intelligent Robots and Systems, San Francisco, CA, USA, 25–30 September 2011; pp. 3260–3267.
18. Lan, X.; Lv, X.; Liu, W.; He, Y.; Zhang, X. Research on robot global path planning based on improved A-star ant colony algorithm. In Proceedings of the 2021 IEEE 5th Advanced Information Technology, Electronic and Automation Control Conference (IAEAC), Xi'an, China, 12–14 March 2021; Volume 5, pp. 613–617.
19. Narayanan, V.; Phillips, M.; Likhachev, M. Anytime safe interval path planning for dynamic environments. In Proceedings of the 2012 IEEE/RSJ International Conference on Intelligent Robots and Systems, Algarve, Portugal, 7–12 October 2012; pp. 4708–4715.
20. Yakovlev, K.; Andreychuk, A.; Stern, R. Revisiting bounded-suboptimal safe interval path planning. In Proceedings of the International Conference on Automated Planning and Scheduling, Nancy, France, 26–30 October 2020; Volume 30, pp. 300–304.
21. Barer, M.; Sharon, G.; Stern, R.; Felner, A. Suboptimal variants of the conflict-based search algorithm for the multi-agent pathfinding problem. In Proceedings of the International Symposium on Combinatorial Search, Prague, Czech Republic, 15–17 August 2014; Volume 5, pp. 19–27.
22. Boyarski, E.; Felner, A.; Stern, R.; Sharon, G.; Betzalel, O.; Tolpin, D.; Shimony, E. Icbs: The improved conflict-based search algorithm for multi-agent path finding. In Proceedings of the International Symposium on Combinatorial Search, Jerusalem, Israel, 11–13 June 2015; Volume 6, pp. 223–225.
23. Li, J.; Ruml, W.; Koenig, S. EECBS: A bounded-suboptimal search for multi-agent path finding. In Proceedings of the AAAI Conference on Artificial Intelligence, New York, NY, USA, 2–9 February 2021; Volume 35, pp. 12353–12362.
24. Ma, H.; Li, J.; Kumar, T.K.; Koenig, S. Lifelong multi-agent path finding for online pickup and delivery tasks. *arXiv* **2017**, arXiv:1705.10868.
25. Greshler, N.; Gordon, O.; Salzman, O.; Shimkin, N. Cooperative multi-agent path finding: Beyond path planning and collision avoidance. In Proceedings of the 2021 International Symposium on Multi-Robot and Multi-Agent Systems (MRS), Cambridge, UK, 4–5 November 2021; pp. 20–28.
26. Sun, S.; Gu, C.; Wan, Q.; Huang, H.; Jia, X. CROTPN based collision-free and deadlock-free path planning of AGVs in logistic center. In Proceedings of the 2018 15th International Conference on

Control, Automation, Robotics and Vision (ICARCV), Singapore, 18–21 November 2018; pp. 1685–1691.

27. Salzman, O.; Stern, R. Research challenges and opportunities in multi-agent path finding and multi-agent pickup and delivery problems. In Proceedings of the 19th International Conference on Autonomous Agents and MultiAgent Systems, Auckland, New Zealand, 9–13 May 2020; pp. 1711–